EISCAT SPACE DEBRIS AFTER THE INTERNATIONAL POLAR YEAR (IPY)

Alan Li
Stanford University, USA, alanli@stanford.edu

Sigrid Close, Jussi Markannen

Abstract

We present results from analysis of space debris data collected with the EISCAT radar. Following the International Polar Year (IPY) in 2007-2009, EISCAT continued to measure space debris with its Svalbard radar. The dataset analyzed consist of more than 48 hours of measurements taken at the end of February 2008. Detection of events was accomplished using the match function, which provides ranges, Doppler velocity and Radar Cross Section (RCS) of detectable debris. The location of the EISCAT radar and the measurements taken allow observation of the January 2007 Chinese anti-satellite (ASAT) test; the subject of the test was the FENGYUN 1C polar-orbiting weather satellite, which was in Sun-synchronous LEO prior to being impacted. These results along with the quality set extracted during the IPY by EISCAT from 2007-2008 are compared to NASA's collision model. NASA's model is known to underestimate the amount of debris that is produced; results skew towards the range of detectable pieces larger than 10 cm in diameter. Piecing together data spanning over a year, we observe the evolution of the debris cloud and total amount of debris generated, including the orbital parameters, velocity and mass distribution of the collision.

1. INTRODUCTION

From March 2007 to March 2009, in an attempt to increase its normal hours of operation, the EISCAT Svalbard Radar (ESR) added its newly constructed space debris receiver to take measurements of orbital debris in addition to its typical ionospheric measurements. From previous ESA contracts between 2000 and 2005, it has been shown to be feasible for EISCAT to detect debris using common transmission but different data processing techniques.

The event described herein involves the Fengyun-1C meteorological spacecraft (International Designator 1999-025A, US satellite number 25730) at an altitude of 850 km and a sun-synchronous orbit inclination of 98.8°. Due to the coincidental occurrence of the January 11th 2007 Chinese ASAT test conducted upon the aforementioned satellite, the data offers insight into the evolution of the debris cloud in the aftermath of the collision. The ESR was thus used to collect data over the course of the year following the event. Formal measurements began in March of 2007 and ended in February of 2008.Beginning in March 2008, bi-weekly measurements were conducted instead. Furthermore, due to problems with the data, only a set of 101 quality days (known as the quality set, QS) with about 95000 events were extracted from March 2007 to February 2008.

We present here approximately 4 days of almost continuous data (breaks in the data resulted from the inclusion of other experiments that utilized the radar). Recording started on February 18, 2008 at 22:00 UT and ended on February 23, 2008 at 11:00 UT. Utilizing the match function (MF), we are able to measure the Doppler velocity and radar cross section (RCS) of detectable debris. Combined with the quality set, the data provide information on the spatial and temporal propagation of the debris cloud.

The paper will compare the measured results with the official Space-Track's Satellite Situation Report (SSR) and RCS data. It is known that NASA's model for this particular collision underestimates the amount of debris produced (refer to [1]). Further comparisons with NASA's official collision model will also be made. In particular, we observe the velocity, orbital parameters and mass distribution of the debris cloud.

2. DETECTION AND PARAMETER ESTIMATION

The EISCAT Svalbard radar, located at 78.2°N, 16°E consisting of 2 dishes (32m and 42m) was tuned to the following parameters at the time of debris detection: a transmission frequency of 499.85 MHz, a transmission gain of 43.9 dB, and a transmission power of 0.9 MW. The system temperature was estimated to be 70 K. The radar transmits with the

42m and receives with the 32m in a bi-static configuration. For a detailed account of the radar setup, please refer to [2] and [3]. Figure 1 shows two 3750 μs interpulse periods with both transmit and receive signals where a detection event is evident in the received portion. The radar beam crosses the debris ring twice per day, and although the transmit and receive nature of the radar allows for unobservable gaps in altitude, the resulting debris was mostly focused at an altitude close to 850 km, which is in the middle of one of the observable zones (700 to 1100 km range).

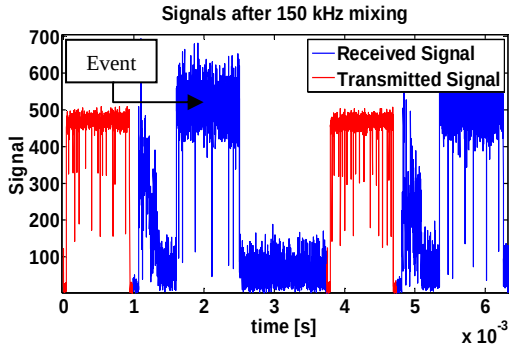

Figure 1. Transmit and receive of radar signal color-coded for transmit and receive (absolute value) signal by the radar. The return contains an evident pulse-form within that signifies a detection event.

Because of the large amount of data, the following process was used to trigger on detection. The raw signal is first put through a convolution with a trigger threshold of approximately 20 dB with zero initial Doppler. As such, at a range of 800 km, the minimum RCS detectable approximates to about 10 mm^2. The resulting locations that triggered are then subjected to further detailed analysis.

We use the match function described by

$$MF(v, R_j) = \frac{\left|\sum_n z_n \bar{x}_{n-j} e^{i2\pi \frac{v}{\lambda/2} n\tau_s}\right|}{\|x\|} \qquad [1]$$

otherwise known as the Radar Ambiguity Function in literature to determine the range and velocity of the detected object. Here R_j is a particular range, z the received signal, x the transmitted signal, v the velocity of the object, λ the wavelength, and τ_s the sampling interval. In practice, however, one uses

$$MF(v, R_j) = \frac{\max\left[DFT\left(\langle z_n, \bar{x}_{n-j}\rangle\right)\right]}{\|x\|} \qquad [2]$$

where DFT is the discrete fourier transform. Thus one has to span the space in range only as opposed to both range and frequency. A smaller frequency range can be specified to search for the maximum that will directly give the Doppler velocity. The corresponding maximum MF result is shown in Figure 2 (frequency information is hidden in this case). As can be seen, the maximum occurs at a range of 800 km where we would expect to see debris.

With the maximum MF, one can get the Energy to Noise Ratio (ENR) or Signal to Noise Ratio (SNR) based upon the variance of the noise in the received signal.

$$\mathrm{ENR} \sim \frac{\max_{v,R} \mathrm{MF}^2}{\sigma_{\mathrm{noise}}{}^2} \qquad [3]$$

A cutoff needs to be specified in order to limit the amount of detections one encounters while analyzing the data. Since the noise variance was observed to stay near the range of 1000 to 1300 W in terms of power received, a maximum MF can be specified instead. As such, an ENR cutoff of approximately 20 dB was set.

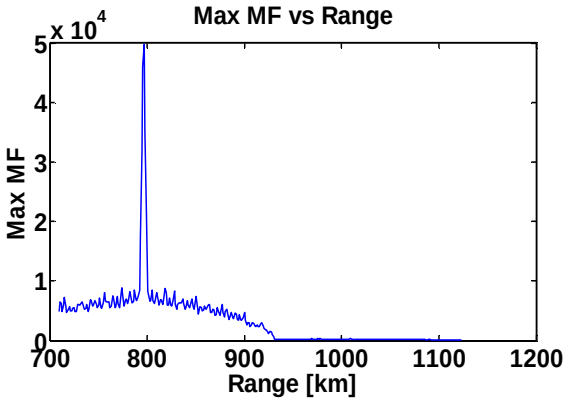

Figure 2. Maximum MF per range slice for the signal received in Figure 1.

This result can then be used with the radar equation to get the RCS of the detected object and furthermore an estimate on the size. Because the offset angle φ is unknown, we have to assume the largest gain, and thus the resulting RCS is skewed towards the minimum size. The RCS is defined as

$$RCS = \frac{(4\pi)^3 k_B T_{sys} R^4 ENR}{G(\phi)^2 \lambda^2 P_x D T_c} \qquad [4]$$

where k_B is the Boltzmann constant, T_{sys} the system temperature, R the range, ENR the energy to noise ratio, G the gain of the antenna, λ the wavelength, P_x

the transmitted power, D the duty cycle, and T_c the coherent integration time.

Furthermore, by using the Raleigh approximation that the object is spherical in shape, one can estimate the diameter. Because true debris particles are not perfect spheres, the result is only approximate and is given by

$$\frac{RCS}{\frac{1}{4}\pi d^2} = 9\left(\frac{\pi d}{\lambda}\right)^4 \qquad when\ d < \frac{\lambda}{\pi\sqrt{3}}$$
$$\frac{RCS}{\frac{1}{4}\pi d^2} = 1 \qquad when\ d > \frac{\lambda}{\pi\sqrt{3}} \qquad [5]$$

where d is the diameter of the object.

Please note that we do not use the "fast" version of the FFT as described in [3] since we were only analyzing a few days' worth of data, and so did not have to deal with the discontinuity artifacts apparent with the Doppler velocity that results from using the fast FFT.

3. DATA

We will focus only on the 2nd altitude range (approximately 700 to 1100 km) since it is where most of the resulting debris from the ASAT test lie. As mentioned before, certain files within the 1.5 terabytes of data are triggered when the initial threshold has been surpassed. These files are then subjected to further analysis as detailed in the previous section such that each file is segmented into 3 portions of 0.24 seconds each. Each portion is then put through the coherent integration and match function processes so that one may get back the ENR, RCS, Doppler and ranges.

From Figure 3b, one can see that the debris "hits" are obvious due to the range of colors starting from a low SNR, increasing to a larger SNR, and then decreasing again (lowest observed at 22.9 dB and the largest at 80 dB). These detections also exhibit the easily identifiable behavior of being vertically aligned. However, it is easier to write an algorithm for detection if we look at a different view of the same dataset.

Despite the noise, Figure 4b actually displays what are long streaks in detection that is much easier to detect by an algorithm. As well, most of these streaks lie in the (-)2000 to (-)4000 Hz regime corresponding to orbital velocities required to maintain such an orbit. A simple linear regression detection test was utilized to highlight these streaks with a regression R > 0.925 indicating a detected straight line.

Two limitations of the algorithm include 1) the frequencies tend to jump more frequently when they exceed 5000 Hz (or below -5000 Hz) and 2) the detection algorithm works more robustly for detections that exceed 5 continuous hits. As such, the algorithm is only able to accurately detect approximately 90% of all hits that fit under these criteria. For our case, we determine that a detection that lasts 0.72 seconds (3 continuous hits in the same frequency regime) to be considered a positive response. Thus the algorithm is unable to incorporate such a short burst of detection since noise starts to filter in.

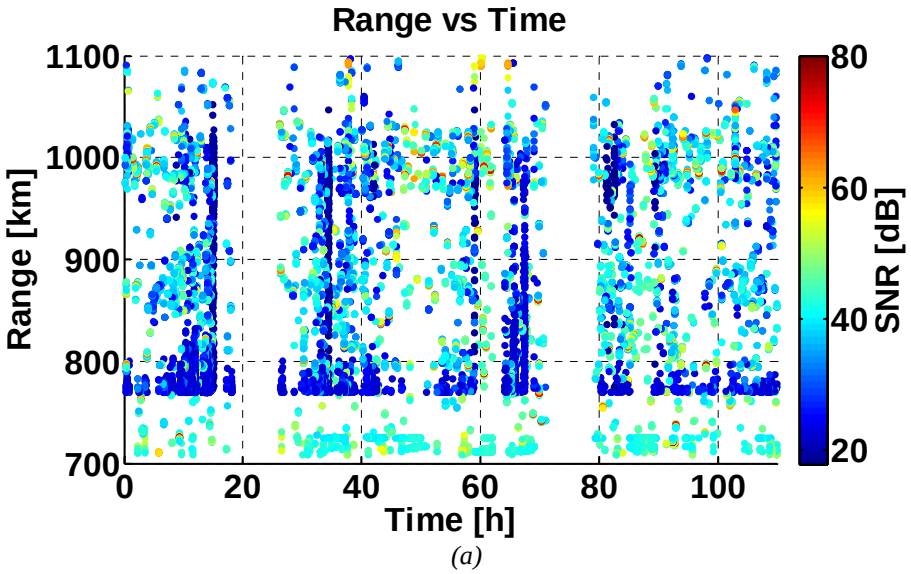

(a)

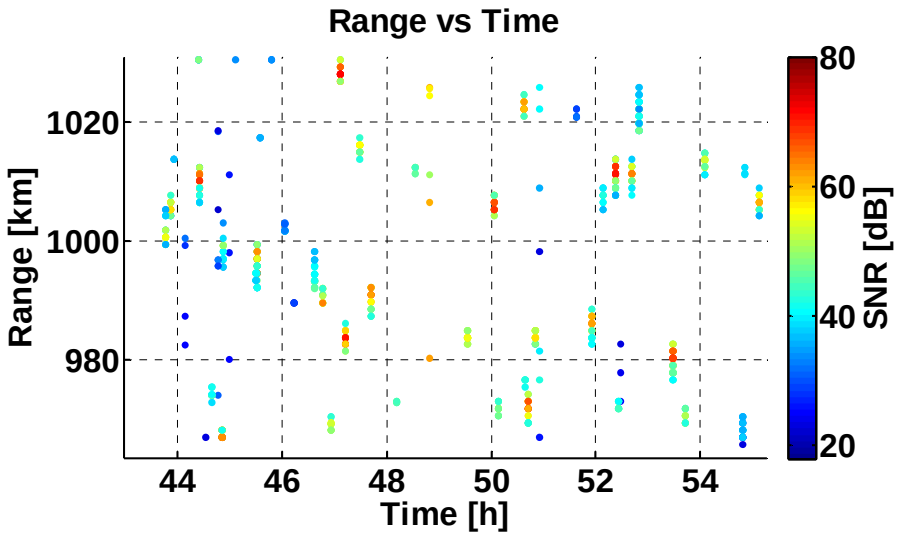

(b)

Figure 3. (a) Range vs time for the 2nd altitude range (700 to 1100 km) color-coded for SNR for the entire detection period of 110 hours. (b) A focused sample of Figure 3a that highlights detection of debris.

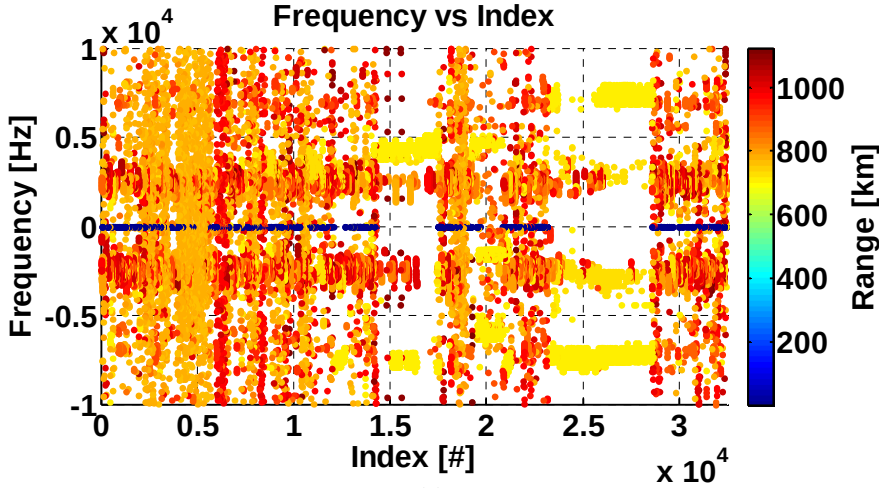

(a)

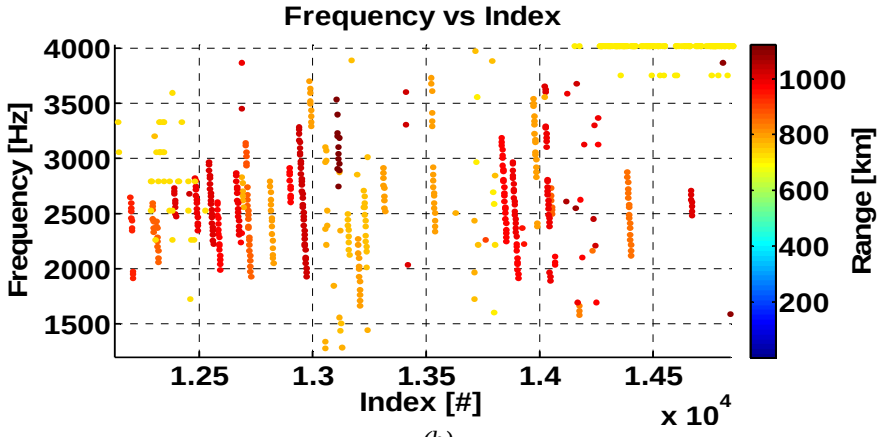

(b)

Figure 4.(a) Frequency vs detection index for the 2nd altitude range (700 to 1100 km) color-coded for range for the entire detection period of 110 hours. The blue colored points at zero frequency indicate junk signals that have been thrown out. (b) A focused sample of Figure 4a that highlights detection of debris.

Without the noise, one can see a much more clearly defined picture of the debris profile. The FENGYUN ASAT event can be seen in Figure 5 from the increase of debris signatures around hours 15 and 38 (corresponding to Feb 19, 13:00 UT and Feb 20, 12:00 UT). Figure 6 gives the associated Doppler detections without the noise.

To relate the detected frequency to Doppler velocity, we use

$$F_d \approx 2v\frac{F_t}{c} \qquad [6]$$

where F_d is the Doppler frequency, F_t the observed frequency, v the velocity, and c the speed of light.

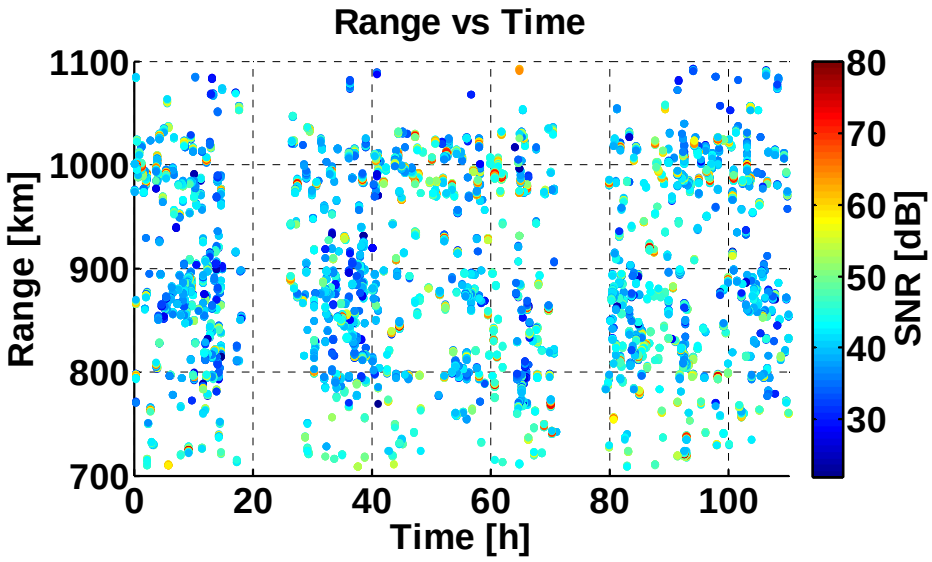

Figure 5. Range vs time color-coded for SNR for a filtered dataset.

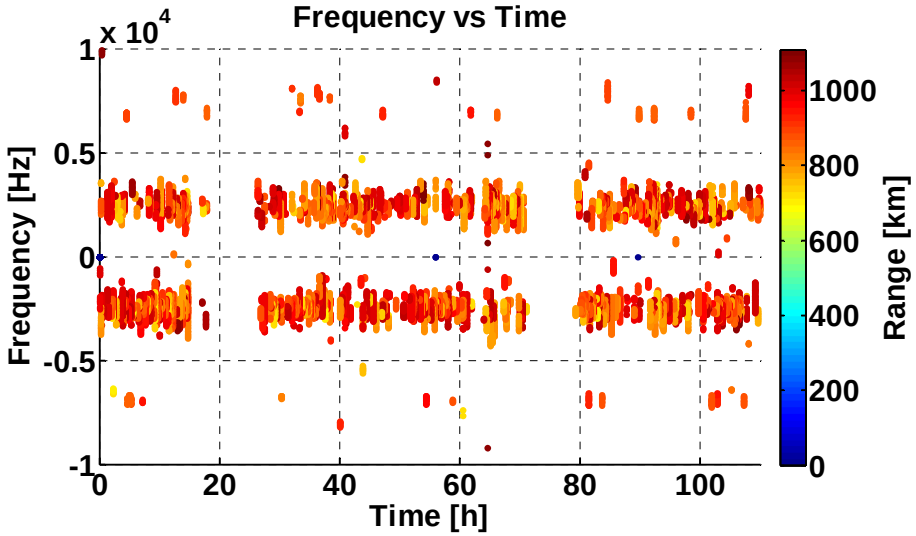

Figure 6. Frequency vs time color-coded for range for a filtered dataset.

This would give most of the velocities observed to be approximately 0.8 km/s. However, this is only the observed velocity along the radar beam. For comparison, if one assumes a sun-synchronous orbit of approximately 98.5 degrees with little to no eccentricity, the calculated velocity does match the observed values.

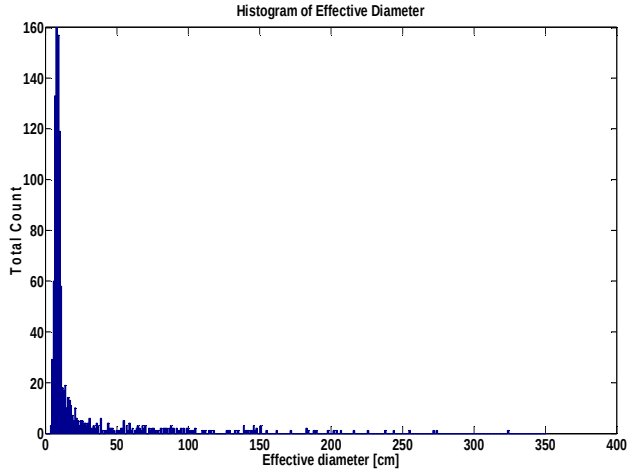

Figure 7. Histogram of effective diameter throughout the entire detection period.

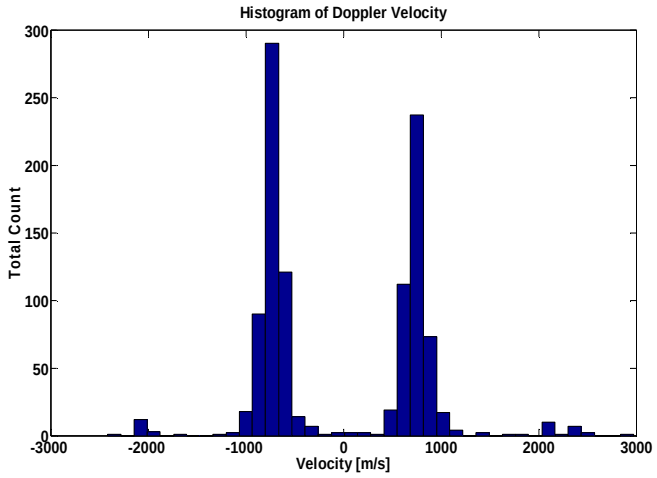

Figure 8. Histogram of velocity distribution throughout the entire detection period.

Overall, comparing the debris profile from Figure 5 with previous measurements shows that a year after the initial breakup event, although the debris ring has definitely expanded beyond its original parameters, a large number of debris can still be found close to its previous breakup orbital elements. It is then possible to construct histograms that reflect the properties of the data. As we can see in Figure 7, most debris possess an effective diameter of about 6 to 11 cm. The steady decrease of debris pieces below 8 cm in diameter is evident in other radars as well and is attributed to the fact that the radar is not sensitive enough to pick up smaller pieces from the noise [1]. The velocity distribution, as shown in Figure 8 also follows the expected trend of being centered about 0.8 and -0.8 km/s respectively.

4. COMPARISONS

We will now examine the overall QS taken starting from the March 13, 2007 to compare the results to the NASA fragmentation model. Because of the nature of the EISCAT radar passing through the debris ring twice per day with no inertial tracking, there is no guarantee that we will observe the same piece of debris throughout multiple passes. As such, we are only able to put forth a statistical analysis of the observed environment.

In Figure 9, which depicts the debris profile for various points in time starting from March 13, 2007, we can distinctly see two bands at approximately 7 and 12 UT that marks the debris ring resulting from the ASAT test. The ring starts as a condensed strip but expands over time. However, in order to maximize the amount of FENGYUN debris collected, it is possible to choose certain regions such as early on during the detection process and when the pinch point of the debris ring passes over the radar.

Figure 10 shows the comparison between the official RCS data given by the SSR and data collected by EISCAT. The most pronounced difference between the two is that the RCS data shows the debris profile lying mostly above the official NASA Collision Model, while the EISCAT data shows it dipping under. In particular, the RCS data shows a drastic increase in cumulative number when the debris sizes are larger. One explanation for this goes back to equation 4, where we stated that we did not know the offset angle, and thus had to assume a maximum gain. This would skew all the data collected by EISCAT towards smaller RCS, and hence smaller diameters. We see that although the two profiles are on opposite sides of the linear NASA Model, they both follow the same shape. To bring the EISCAT data to correlate with the observed RCS data, we would have to reduce the gain by a factor of 3. Although this would be a good fit for debris sizes smaller than 2 m in diameter, it does predict much larger debris over 2 m.

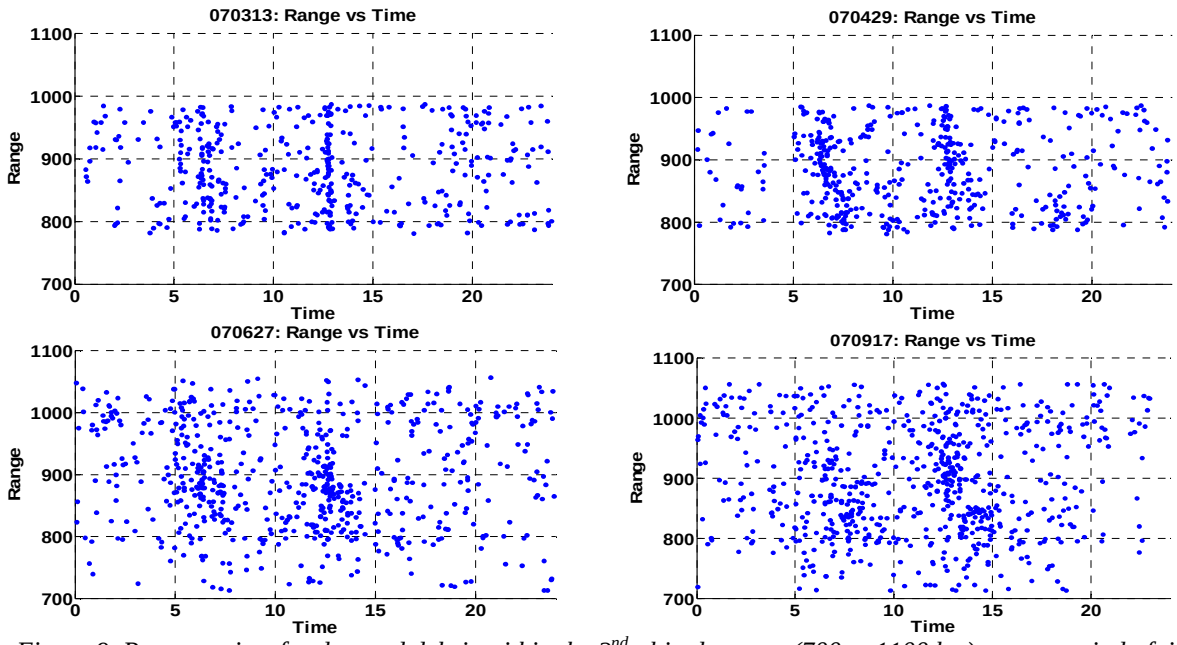

Figure 9. Range vs time for detected debris within the 2nd altitude range (700 to 1100 km) over a period of time

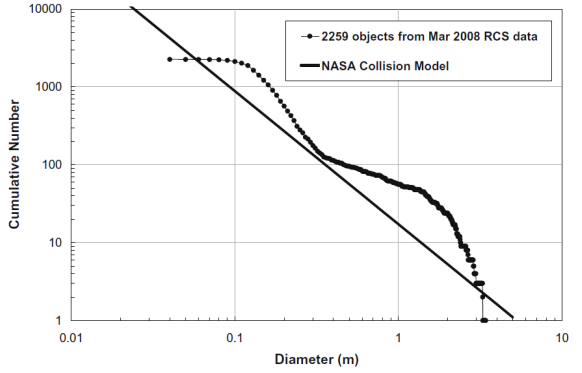

(a)

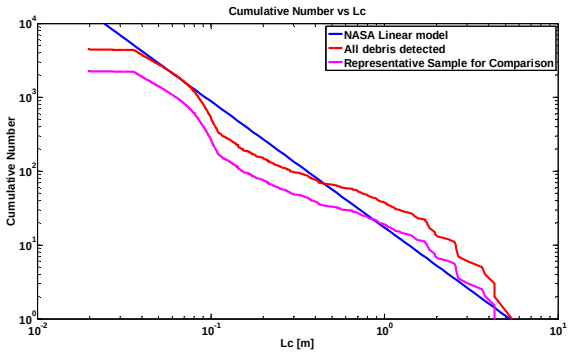

(b)

Figure 10. (a) Comparison between official SSR RCS data and NASA collision model. (b) Comparison between NASA collision model and EISCAT data. The red line in represents all events and the magenta line takes 2259 of those events so as to create a comparison between the official SSR RCS data.

Figure 11 shows the same debris profile as in Figure 10b, but now the NASA exponential model (refer to [6] for details) given by,

$$N(L_c) = SF \cdot [F_1(L_c) + F_2(L_c)] \qquad [7]$$

where

$$F_1(L_c) = a_5 \cdot {L_c}^{a_6} \qquad [8]$$

and

$$F_2(L_c) = a_1 \cdot {L_c}^{a_2} \cdot \exp(-a_3 \cdot {L_c}^{a_4}) \qquad [9]$$

is fitted to the magenta curve. $N(L_c)$ is the cumulative number of objects greater than or equal to the characteristic length L_c, the ensemble a_i are the fit coefficients, and SF is the multiplicative scaling factor (1 in our case). The fit is a fairly accurate one as the values chosen for a_i for i=1,6 are as follows: [40,-0.43,0.9,0.75,0.01,-4]. The method for choosing such numbers was done here by iterative methods. Although there are other techniques that utilize a formal non-linear least squares fitting procedure, again the curve fitting method is data driven and not dependent on any characteristics of the collision itself.

Another analysis can be done to determine the inclination of the debris profile. However, due to the limited data, one has to assume a near zero eccentricity (most eccentricities are below 0.04) to back out inclination from a measured range and velocity. This assumption, however, does have

consequences in the fact that the inclination profile, although sharing the same peak as official RCS data, will be slightly different in its distribution. The results are shown in Figure 12. Due to the nature of the detection process, it is feasible to only look at a representative sample of the total number of detections. To achieve this, one needs to segment off very narrow bands of the debris ring so as to avoid noise from other irrelevant signals.

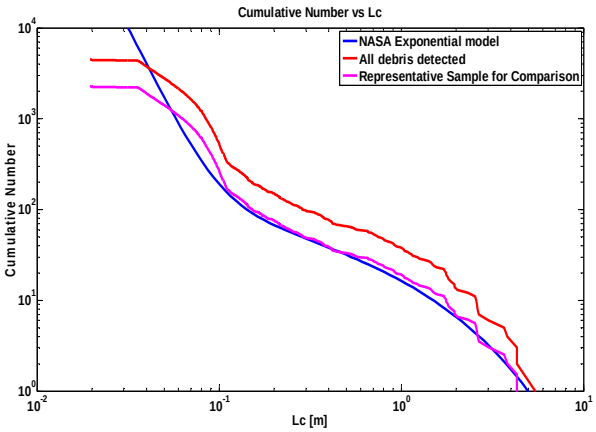

Figure 11. NASA exponential model fitted to EISCAT representative sample curve.

Figure 12 shows that apart that catalogued fragments and measurements by EISCAT do share a peak inclination of approximately 99°. However, the EISCAT data exhibits a much gentler distribution, particularly skewed towards the lower inclinations, than that exhibited by the catalogue. Adding more data points into the process does not remedy this issue, but instead adds additional noise that further smoothes the curve.

Because it is difficult to actually calculate the area to mass ratios without constant tracking of a piece of debris, we have executed Monte Carlo simulations to determine the masses of the debris cloud given the official FENGYUN area to mass (A/M) ratios. As shown in Figure 13, we can see a Gaussian distribution that comes from the official NASA collision model. The masses from the RCS A/M data however show that they are not so well-behaved. Because of the FENGYUN collision being particularly skewed towards high area to mass ratios, the masses themselves are skewed towards lower values.

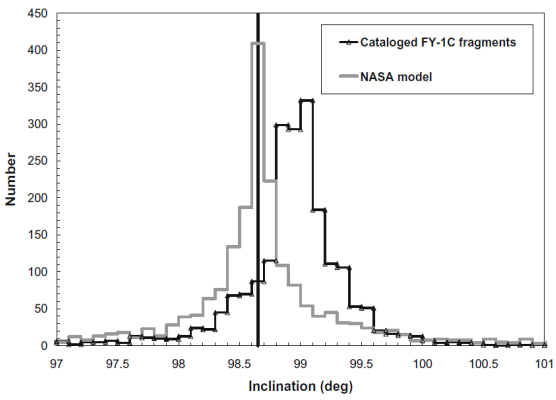

(a)

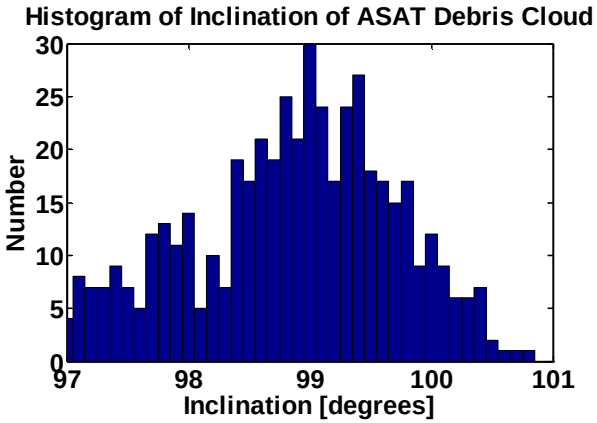

(b)

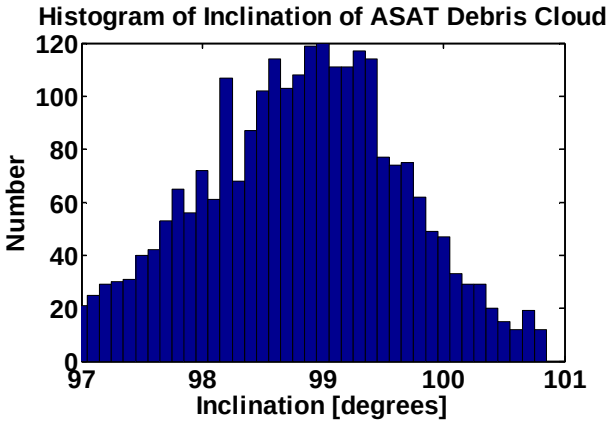

(c)

Figure 12. (a) Comparison between NASA model and catalogued fragments. (b) Inclination data from first 10 days of EISCAT data. (c) Inclination data from additional days in EISCAT data. Due to noise, the curve is smoothed over, but still exhibits a peak at about 99 degrees.

Although higher area to mass ratios do shorten the lifetime of debris, collision damage might be more severe due to the increased number of larger debris.

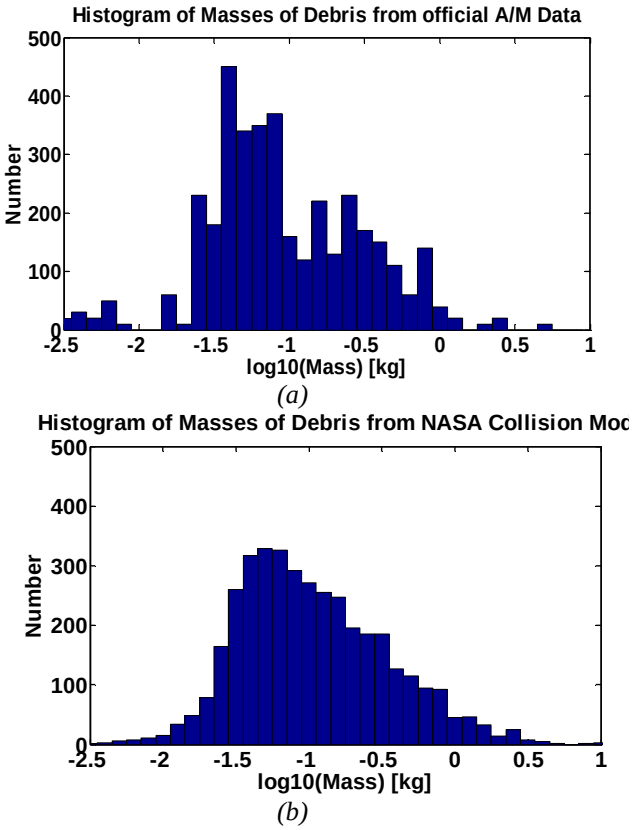

Figure 13. (a) Histogram of masses of debris between 10 and 20 cm in size from Monte Carlo simulation utilizing official RCS A/M data. (b) Histogram of masses of debris between 10 and 20 cm in size from Monte Carlo simulation utilization official NASA fragmentation model.

5. CONCLUDING REMARKS

We have described a methodology for debris detection using EISCAT and applied this approach in order to examine the debris profile of the FENGYUN ASAT test. We then studied the entire IPY EISCAT dataset itself to try to form a comparison to the official NASA models and RCS data. Due to the lack of inertial tracking, our efforts here were reduced to more statistical analysis and Monte Carlo methods.

The overall cumulative number of debris was observed to have a similar shape to that of the official set, except for the profile being shifted slightly to the left which was attributed to assuming a high gain when calculating the RCS. The NASA power and exponential fit was seen to be a much better fit of the data than the linear model, although the techniques for finding the correct fit are not based upon the characteristics of the collision itself. The inclinations calculated peaked at the same area as that of the official set but was much smoother due to the addition of debris that was not relevant to the collision itself. Finally the difference between the NASA collision model and the official RCS data in estimating the masses of the debris pieces can be clearly seen. There is a skew towards lower masses but the curve does not follow any Gaussian distribution as the NASA model does.

Because of the uncertainty when dealing with the EISCAT data set as to whether the debris actually originated from the FENGYUN collision or not, future work will look at the correlation between official SSR data with detections made by EISCAT. The resulting profiles after such a comparison might offer a better view of the debris profile after impact, especially towards the smaller sizes.

6. REFERENCES

[1] Liou, J.-C., Johnson, N.L. Characterization of the Catalogued Fengyun-1C Fragments and their long-term effect on the LEO Environment. Advances in Space Research 43, 1407-1405.

[2] Markkanen, J., Lehtinene, M., Landgraf M. Real-time Space Debris Monitoring with EISCAT. Advances in Space Research 35, 1197-1208.

[3] Markkanen, J., Jehn, R., Krag, H. EISCAT space debris during the IPY – A 5000 hour campaign. 5th European Conference on Space Debris, March 2009.

[4] Markkanen J., Postila M. Real-time small-size space debris detection with EISCAT radar facilities, Final Report, ESOC Contract No. 16646/02/D/HK(CS), 2005. On-line as www.sgo.fi/~jussi/spade/FRII_21feb2005.pdf

[5] Markkanen J., Lehtinen M., Huuskonen A., Vaananen, A. Measurements of small-size debris with backscatter of radio Waves, Final Report, ESOC Contract No. 13945/99/D/CD, 2002. On-line as www.sgo.fi/~jussi/spade/FR_16Apr2002.pdf

[6] Anz-Meador, P.D., Matney, M.J. An Assessment of the NASA Explosion Fragmentation Model to 1 mm Characteristic Sizes. Advances in Space Research 34, 987-992.

[7] Johnson, N.L., Stansbery, E.G., Liou, J.-C., et al. The characteristics and consequences of the break-up of the Fengyun-1C spacecraft, Acta Astron., 21, 14, 2008.

[8] Johnson, N.L., Krisko, P.H., Liou, J.-C., Anz-Meador, P.D. NASA's new breakup model of evolve 4.0. Advances in Space Research 28, 1377-1384.

[9] Stansbery, G., Matney, M., Liou, J., Whitlock, D. A comparison of catastrophic on-orbit Collisions. Proceedings of the Advanced Maui Optical and Space Surveillance Technologies Conference, September 17-19, 2008. Ed.: S. Ryan, The Maui Economic Development Board, p.E50